Experimental study of the dynamics of a diode-pumped Nd:YVO_4 laser under periodic modulation of losses

V.J. Pinto Robledo[a], G. Lopez[a], Y. M. Espinosa[a], A.N. Pisarchik[a], R. Jaimes Reátegui[b], and V, Aboites[a]
[a]*Centro de Investigaciones en Optica,*
Loma del Bosque 115, Leon Gto., 37100 Mexico.
e-mail: vpinto@cio.mx
[b]*Universidad de Guadalajara, Centro Universitario de los Lagos,*
Av. Enrique Diaz de Leon s/n Paseos de la montaña Lagos de Moreno Jal. 47460 Mexico.

Recibido el 17 de octubre de 2011; aceptado el 9 de noviembre de 2012

With the aim of developing experiments for teaching dynamics of complex systems and stabilization methods in lasers, we study the dynamics of a diode-pumped Nd:YVO_4 laser under periodic loss modulation produced with an acousto-optic modulator and a function generator. Our goal is stabilization of the laser oscillations in a chosen dynamical state. The results obtained with the rate-equation model for different modulation schemes are in a good agreement with the experiments.

Keywords: Chaos on lasers; laser dynamics; Nd:YVO_4 lasers.

PACS: 05.45.Gg; 95.10.Fh; 42.65.SF

1. Introduction

Compact solid-state lasers are the most important source of laser light widely explored in industry and technology nowadays. These lasers are highly efficient and robust and they can work in diverse industry environments [1]. Nevertheless, at powers medium to high the lasers suffer from dynamical instability and their emission becomes unacceptable in many applications like those requiring high precision, such as micro precision processing of drilling, welding, marking and cutting, rapid prototyping, and so on. Dynamical fluctuations arise from inherent laser dynamics and in some cases are forced by mechanical and thermal effects of strong pumping [2]. Among different active media of compact solid state lasers, a Nd:YVO_4 crystal is widely used laser crystal, because of its larger emission cross section compared with Nd:YAG, higher efficiency in converted pumping energy, and lower lasing threshold. On the other hand, Nd:YVO_4 crystals are birefringent and have anisotropic emission cross section, they suffer from stronger thermal effects than Nd:YAG. Nevertheless, it is one of the best crystals when the pumping is done with diode lasers. Because of the involved laser state lifetimes, Nd:YVO_4 can be modulated at much higher frequencies than Nd:YAG, that makes the laser a good candidate for high speed processing.

Solid state lasers like Nd:YVO_4, Nd:YAG, and Nd:YALF are known as type-B lasers [6,7], which dynamics is regulated by two variables, the optical field and the population inversion. These lasers are usually adiabatically stable. However, they become chaotic if an additional variable is introduced to the system. Unwanted chaos can be caused nonlinear interaction between laser modes, *e.g.*, between longitudinal modes when a second harmonic generation crystal is inserted into the cavity [9]. This so-called "green problem" became relevant with the need to miniaturize cw intracavity frequency doubled solid state lasers. Chaotic lasers have been extensively studied for application in secure communication systems, where information is encoded into chaotic light carriers and then transmitted through optical fibers. The message is decoded in the receiver with another chaotic laser, which is synchronized with the laser in the transmitter [10]. In this area, generation and control of chaotic laser oscillations are very important.

Chaos in a laser can be generated either by direct optical feedback from an external mirror, by parameter modulation [3,4], or by light injection from another laser. As soon as chaos emerges, its control becomes an important problem. Several control methods have been developed to stabilize an unstable periodic orbit embedded into a chaotic attractor. Some of them use parameter modulation, like the OGY (Ott-Grebogi-Yorke) method [14], the others imply the modulation of a system variable, like the Pyragas method [12]. The available modulated parameter can be either the pumping power or the optical losses. The disadvantage of these control methods is that they require a full mathematical description of the underlying nonlinear model of the laser system, since the exact knowledge of the attractor is needed in advance in order to analyze and control the system. In practice, this is a difficult task although feedback control of chaos has been demonstrated in Nd:YAG [4] and other lasers [5].

The simplest method of stabilizing chaotic laser dynamics is the open loop control by applying periodic modulation to a single laser parameter, specifically, to cavity losses as $a = a_0[1 - m\sin(2\pi f_c t)]$, where a and f_c are the modulation amplitude and frequency, respectively. With this method, the weak modulation brings the system to a nearby orbit eventually stabilizing the laser in a periodic orbit. Such non-feedback control can be performed by applying resonant, $f_c = (1/n)f_n$, where $n = 1, 2, ...$, near resonant $f_c \simeq (1/n)f_n$, or nonresonant $f_n \gg f_c$ perturbation, where

f_n is the characteristic or natural frequency of the laser. The nonfeedback nonresonant control can be realized in the form of fast or slow parameter modulation, slow means that the frequency of the control modulation f_c is much smaller than the characteristic laser frequency f_n, *i.e.* $f_c \ll f_n$. Some of these stabilization methods are used to suppress unwanted oscillations of semiconductor laser devices, such as DVD players [16], which are very sensitive to destabilizing unwanted optical feedback, and where harmonic modulation prevents the chaotic output. The same control principles can be applied to diode-pumped solid-state lasers.

In this work, we apply weak modulation to laser losses to observe changes in dynamical states occurring under the modulation. The aim of this study is to distinguish different dynamical states in laser dynamics by varying laser and modulation parameters within accessible ranges. Our study intends to help in didactics of dynamical systems providing visualization of different dynamical regimes. We do not intend a full characterization of the laser dynamics, but just use our setup for the didactic purpose. The paper intents to provide students with the experimental practice besides high theoretical background by offering them to observe complex laser dynamics using the simplest control technique. In such a way, the students get involved into the experimental study working with lasers and collecting time series with a great number of samples through PC-based A/D samplers. They will also improve their skills in programming and data analysis.

2. Modeling

The laser is modeled with the four level rate equations, which assume a single mode lasing. The Nd:YVO_4 is birefringent but it normally oscillates in a preferential polarization, so that we model the oscillation with a single polarization. The four level laser scheme is shown in Fig. 1. As distinct from other models of this laser, the parameters in the model we use [8,15] are closer to real laser parameters.

$$\frac{d\varphi}{dt} = \frac{\varphi}{\tau_r}\left[2\sigma l_g(N_2 - N_1) - \left(\ln\left(\frac{1}{R}\right) + \epsilon\right)\right], \quad (1)$$

$$\frac{dN_2}{dt} = PN_0 - \left(\frac{1}{\tau_{20}} + \frac{1}{\tau_{21}}\right)N_2 - \sigma c(N_2 - N_1)\varphi, \quad (2)$$

$$\frac{dN_1}{dt} = -\frac{N_{10}}{\tau_{10}} + \frac{N_2}{\tau_{21}} + \sigma c\varphi(N_2 - N_1), \quad (3)$$

$$\frac{N_0}{dt} = \frac{N_{20}}{\tau_{20}} + \frac{N_1}{\tau_{10}} - PN_0, \quad (4)$$

where φ is the photon density, N_i is the population density of the laser level $(i = 1, 2, 0)$, σ is the laser stimulated emission cross section, t_{ij} is the decay time of transition between levels i and j. We neglect the population of level 3 assuming that all atoms pass to level 2 very fast without emission. l_g is the active medium length, c is the light velocity, R is the reflectivity of the output coupler, P is the pumping rate. The round-trip cavity loss is defined as

$$\epsilon = L + \gamma(t), \quad (5)$$

where L is the static loss and $\gamma(t)$ is the modulating function. The parameters used for Nd:YVO_4 are $\sigma = 2.5\times10^{-18}$ cm^2, $\tau_{21} = 90$ μs, $L = .04$, $N_t = 1.37\times10^{20}$ cm^{-3}, and the (approximated values of $\tau_{20} = 3.9\times10^{-4}$ s, $\tau_{10} = 3\times10^{-8}$ s). The parameters of the resonator are given in the next section. Using the above parameters of our Nd:YVO_4 laser, we numerically solve the set of equations using the fourth order Runge-Kutta method in order to obtain time series of the laser output intensity.

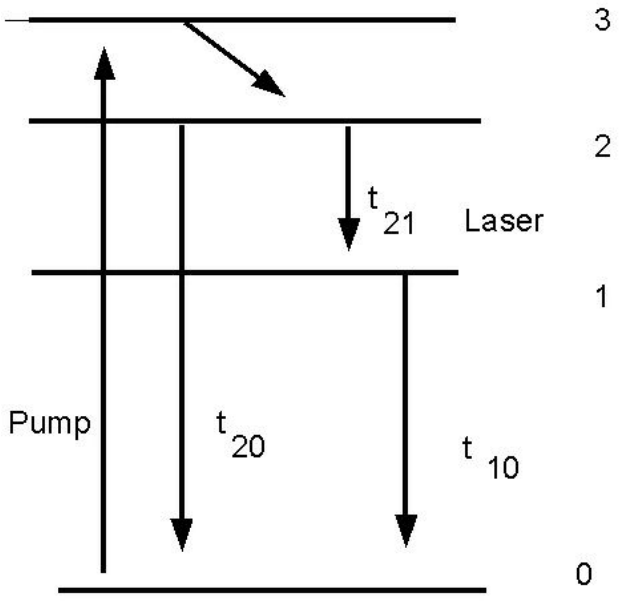

FIGURE 1. Energy diagram for the laser modeling.

3. Experimental

The experimental set-up is schematically shown in Fig. 2. We use a 2×2×3 (mm) Nd:YVO_4 laser crystal end-pumped by a fiber coupled semiconductor laser at a pump wavelength of 809 nm (LD). The maximum pump power is 5W and the polarization of the pump beam is aligned with the crystal c axis. The resonator consists in a mirror (M1) with high reflectivity at 1064 nm and AR coating to the pump radiation and the second mirror (M2) with reflectivity of 94% as output coupler. Both mirrors are flat, the resonator length is 125 mm, the pump radiation is focused by convex lens (L) with 25 mm focal length. The cavity loss is modulated with an acousto-optic modulator (AOM) Intraaction mod AOM405AF1. The modulation signal from a signal generator (SG) is applied to the driver of an acousto-optic modulator (RF). The use of flat mirrors make a near unstable resonator, but the thermal lens in the laser crystal generated by the pumping ensure that the resonator works well in a stable region. The resonator is made to work in TEM_{00} mode using a small aperture. Power

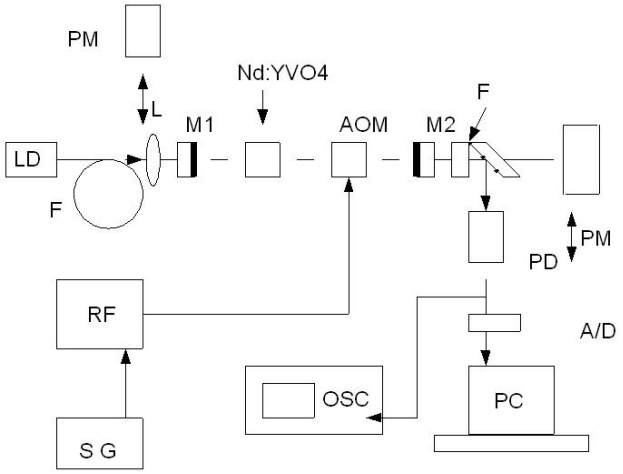

FIGURE 2. Experimental setup.

measurements of the pumping beam and the laser output are performed with a Nova laser power meter (PM) from Ophir Instruments. With these values, the characteristic time is $\tau_c = nl/(1-R)c$, $\tau_c \simeq 13.6$ ns. The laser output pass through a 1064-nm pass band filter (F) and directed to a photodiode (PD), then the signal is displayed on an oscilloscope and simultaneously recorded with an A/D card on a PC running Labview software to perform post time series analysis, such as Fourier spectrum, Lyapunov exponents, and visualization of a phase diagrams in order to recognize chaos [7].

In visualizing time series it is sometimes difficult to recognize meaningful patterns, especially when the waveforms are not periodic but rather quasiperiodic, *i.e.*, when the oscillations have multiple periods. The analyses of more complex patterns, like chaos, is even more difficult, it requires special mathematical techniques, like Fourier analysis, which can be easily performed with PC or as a built-in mathematical function in modern digital oscilloscopes. Although the Fourier analysis is very important, the spectrum recognition by eye is also difficult. In the case of chaotic output, it is sometimes difficult to distinguish chaos from simple noise. The Fourier analysis shows that chaotic series have a bell shape spectrum, but in some cases it is better to use other tools, like Lyapunov exponents, which measure the system sensitivity to a change in initial conditions. If the system is allowed to evolve from slightly different initial states, x and $x+\epsilon$, after n interactions their divergence may be characterized approximately as [7] $\epsilon(n) \approx \epsilon e^{\lambda n}$, where λ is the Lyapunov exponent, defined as

$$\lambda = \lim_{n\to\infty} \frac{1}{n} \sum_{i=0}^{n-1} \log_e |f'(x)| \,. \qquad (6)$$

If λ is negative, the trajectories converge and the evolution is not chaotic, but if λ is positive, nearby trajectories diverge and the system becomes chaotic. Although this concept is very useful, numerical estimations of the Lyapunov exponents from time series is rather a sophisticated task. We calculate the Lyapunov exponents using the algorithm from Ref. 11.

4. Results and Discussion

In this work, we study the laser dynamics using time series analysis numerically and experimentally and compare the results. In the experiment, we observe the dynamics that allows us to see immediate changes in states while adjusting the laser parameters. In order to ease visualization, we construct phase diagrams with I(t) vs dI(t)/dt, where we can see the transition from a fixed point to closed orbits and a more dense type of trajectories, and in some cases we recognize chaos with its characteristics. These phase diagrams are intended to be an important visual tool for analyzing one-dimensional time series, but from the dynamics point of view they are not a true dynamical phase state, since the last is multi-dimensional space, not accessible from the experiment. The characterization of the saved time series is made in a posterior numerical analysis.

The laser without modulation works in a cw regime (fixed point) with the output power being in the range of tens of mW. Near the threshold these lasers exhibit instabilities due to small perturbations due to natural relaxation oscillations, which result from the interplay between the population inversion and the photon density in the laser medium. Their characteristic frequency depends on the pump power and static losses. Figure 3 shows the variation of the relaxation frequency with the laser pumping power. Near the threshold, the relaxation oscillations range from 80 to 160 kHz. These values are consistent with theoretical values obtained by using the cavity parameters and $f_n = \sqrt{(r-1)/\tau_c\tau - (r/2\tau)^2}$ [8], where $r = P/P_{th}$ is the normalized pumping power, P is the pump power, P_{th} is the pumping threshold, t_c is the cavity decay time, and τ is the laser level decay. With the pumping power near threshold $r \simeq 1.049$, we have $f_n \simeq 200$ KHz, nevertheless, with stronger pumping this frequency grows up rapidly. In the experiments, this frequency sets the lower

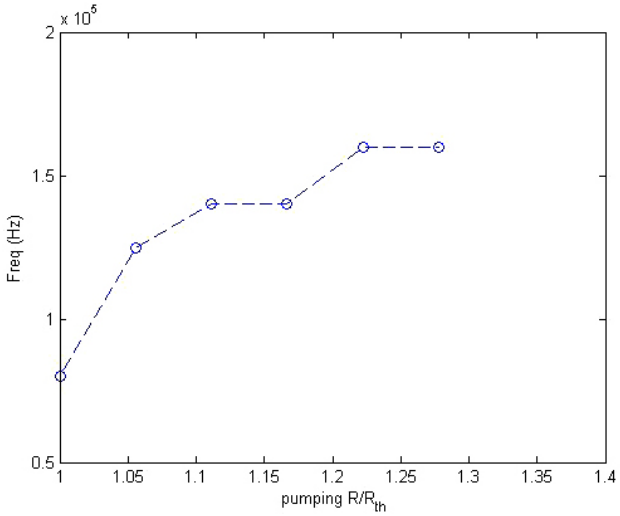

FIGURE 3. Experimental measurement of relaxation oscillation frequencies.

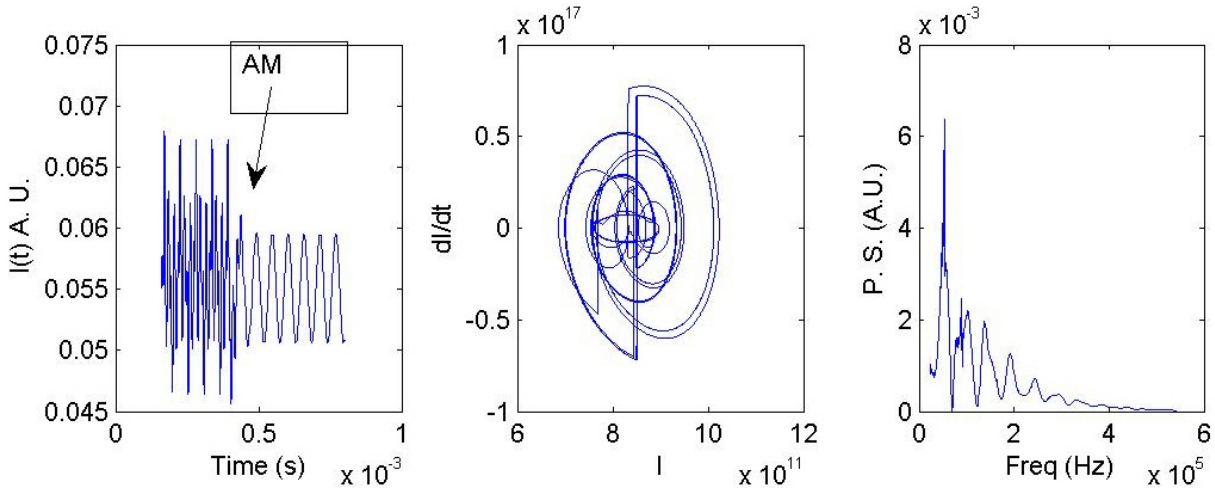

FIGURE 4. Modeled time series for sinus wave control signals.

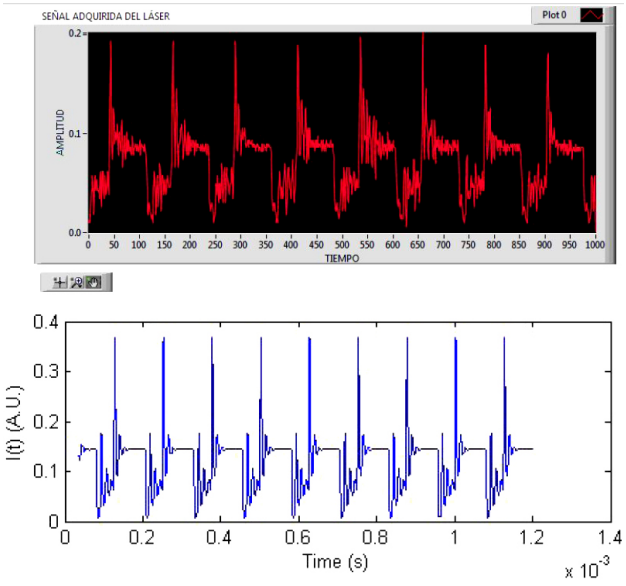

FIGURE 5. Experimental and modeled laser output.

limit in the time scale of the observed changes. Thus, we restrict the measurements to the lowest pumping, where the frequency is low enough to enable time series measurements with a relatively low resolution.

Pumping above the lasing threshold, the laser output is stable in a fixed point, but instabilities may occur if there is some optical feedback or some noise in the pumping. In our case, the instabilities are caused by the loss variation by an intracavity acousto-optic modulator. Even though the modulation used is very small, the laser output is modified by the modulation. Modulating with a sinus wave, the laser output follows the modulation signal, thus for low frequencies (few kHz) the output is a sinus wave (Fig. 4). In this case of modulation, visible changes in the dynamics occur only for higher frequencies. Nevertheless, some more complicated dynamics is set when we modulate the losses with other waveforms, as *e.g.* those shown in Figs. 5, 7, 8, where the modulation function is a square wave. In the case of very low frequencies and small modulation, the laser exhibits natural relaxation oscillations at each cycle. Increasing the modulation frequency, these oscillations are not damped and laser output oscillate in a more complex manner, like a collection of periodic orbits. For higher frequencies, these multi-periodic outputs change to patterns like chaos shown in Fig. 6. Chaos is recognized by the wide spectrum and also by the positive Lyapunov exponent.

The time series obtained with the model are in agreement with the experimental waveforms. Although there are some

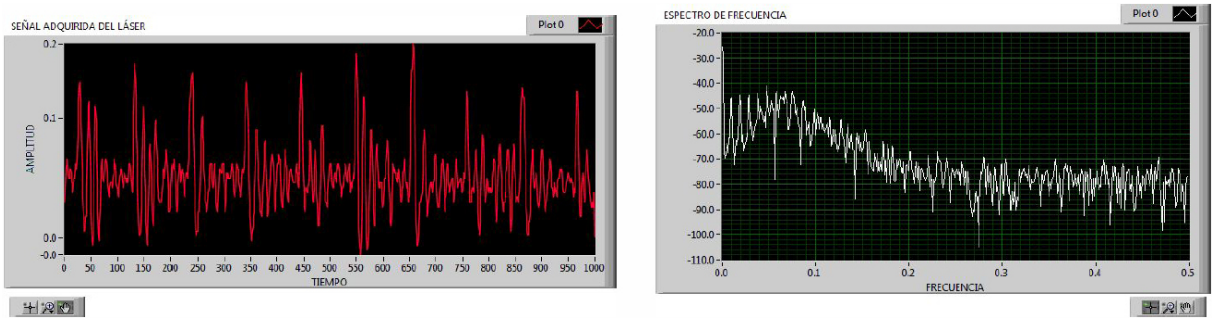

FIGURE 6. Laser Intensity and power spectrum (Arb. Units) with slight chaotic contribution, Lyapunov exponent λ=0.402.

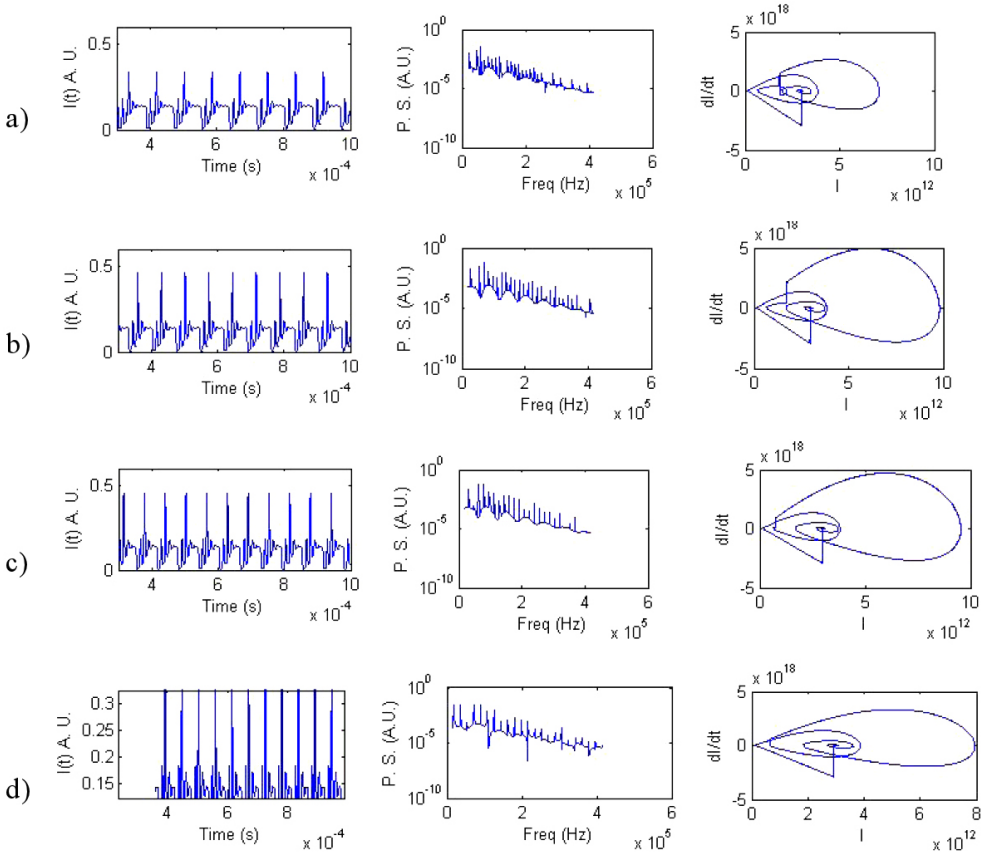

FIGURE 7. Modeled time series for different modulation frequencies, Intensity (A. U., and time), Power spectrum (A.U.), and phase diagrams, a) 12 KHz, b) 14 KHz, c) 16 KHz, d) 18 KHz.

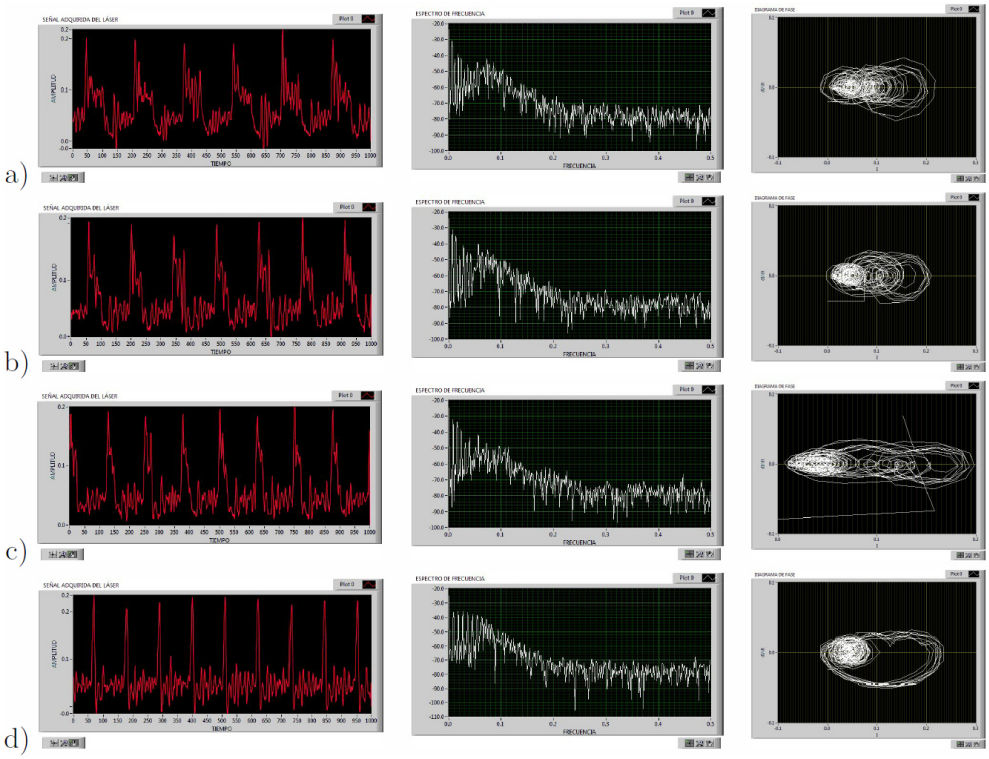

FIGURE 8. Experimental time series for different modulation frequencies , Intensity (A. U., and time), Power spectrum (A.U.), and phase diagrams. a) 12 KHz, b) 14 KHz, c) 16 KHz, d) 18 KHz.

limitations of the model, perhaps the most important would be the limitation of modeling only one mode whilst in the experiment several modes may oscillate. Since it is easier to have a emission with several modes, the oscillation in a number of modes increases the complexity of the output waveforms, generating chaos in some cases, while in a single-mode model it is harder to find chaos. Another limitation is that noise in the model is not taken into account. However, in practical situations, noise is very a important factor because it can modify dynamics. Even though the model can accurately describe the laser output, there are also some limitations for the accuracy in the input data. It is found that the dynamics is very sensitive to some parameters, such as internal reflectivity, cavity length, internal losses, and so on, which are sometimes difficult to know with great accuracy. When comparing the experimental waveforms with the results of the numerical simulations, even if the time series made for a great number of points, only a few of the last data are shown in the graphs in order to see the stabilized output after the initial transitory at the start up of the laser.

5. Conclusions

In order to help students to understand dynamics of complex systems in the fields of optics and lasers, the dynamics of a Nd:YVO_4 laser under low frequency loss modulation have been studied both numerically and experimentally. The modulation produces a very rich dynamics which can be experimentally visualized and analyzed. The experimental setup can be used to further study of control methods to stabilize the laser on particular states and to study conditions for which the laser falls into chaotic states. The results of numerical simulations display a qualitative agreement with the experiment. The future work involves the observation of the effect of modulation on the laser dynamics at much higher frequencies.

Acknowledgments

G.L.M. and Y.M.E., the students from Instituto Tecnologico de Tuxtla Gutierrez, thank to the Delfin program of CONACYT for the financial support in their stays in Centro de Investigaciones en Optica to perform this work.

1. W. Koechner, *Solid State Laser Engineering*, (Springer 1998).
2. R. Scheps, *Introduction to Laser Diode-Pumped Solid State Lasers* (U Press 2006).
3. C. Bracikowski and R. Roy, *Chaos* **1** (1991) 49–64.
4. R. Meucci, R. McAllister, and R. Roy, *Phys. Rev. E* **66** (2002) 026216.
5. A. Ahlborn and U. Parlitz, *Opt. Lett.* **31** (2006) 465–467.
6. C. O. Weiss and R. Vilaseca, *Dynamics of Lasers, Nonlinear Systems*, ed. H.-Schuster, (VCH 1991)
7. R. C. Hilborn, *Chaos and Nonlinear Dynamics*, (Oxford UP, reprint 2004)
8. A. Yariv, *Optical Electronics* (HRW third edition 1985).
9. G. Kociuba, N. R. Heckenberg, and A. G. White, *Phys. Rev. 64* (2001) 056220.
10. A. Uchida , M. Shinozuka, T. Ogawa, and F. Kannari, *Opt. Lett.* **24** (1999) 890.
11. J.C. Sprott, *Chaos and Time Series Analysis* (Oxford U. P. 2009).
12. K. Pyragas, F. Lange, T. Letz, J. Parisi, A. Kittel, *Physical Review E* **61** (2000) 3721.
13. B.K. Goswami and A. N. Pisarchik, *Int. J. Bif. Chaos* **18** (2008) 1645–1673.
14. E. Ott, C. Grebogy, and J. A. Yorke, *Phys. Rev. Lett.* **64** (1990) 196.
15. D. Y. Tang *et. al.*, *Opt. Lett.* **28** (2003) 326.
16. J. Ohtsubo, *Semiconductor Lasers* (Springer Series in Optical Sciences 2008).